Journal of Molecular Catalysis A: Chemical 329 (2010) 86–95

Contents lists available at ScienceDirect

Journal of Molecular Catalysis A: Chemical

journal homepage: www.elsevier.com/locate/molcata

# Stabilizing nanoparticle catalysts in imidazolium-based ionic liquids: A comparative study

Priyabrat Dash, Sarah M. Miller, Robert W.J. Scott*

*Department of Chemistry, University of Saskatchewan, 110 Science Place, Saskatoon, Saskatchewan, Canada*

ARTICLE INFO

*Article history:*
Received 24 March 2010
Received in revised form 17 June 2010
Accepted 24 June 2010
Available online 1 July 2010

*Keywords:*
Ionic liquids
Nanoparticles
Catalysis

ABSTRACT

Room temperature imidazolium-based ionic liquids such as 1-butyl-3-methylimidazolium hexafluorophosphate ($BMIMPF_6$) have been used as effective liquid media for the synthesis of pure Au and bimetallic PdAu nanoparticles by direct synthesis and phase-transfer methods. The mode-of-stability, long-term stability, and long lifetimes of these ionic-liquid supported nanoparticle catalysts, all of which are important factors in determining the overall "greenness" of such materials, were investigated. Four different stabilizing systems in $BMIMPF_6$ ILs were investigated: poly(vinylpyrrolidone) (PVP), 1-methylimidazole, 1-(2′-aminoethyl)-3-methylimidazolium hexafluorophosphate, and pure $BMIMPF_6$ IL with the absence of a secondary stabilizer. The stability of pure Au nanoparticles synthesized by the above four stabilizers was studied using UV–vis spectroscopy and transmission electron microscopy (TEM). It was found that PVP-stabilized nanoparticles were the most stable to aggregation. The catalytic activity of the resulting PdAu nanoparticles was examined for the hydrogenation of 1,3-cyclooctadiene and 3-buten-1-ol across all of the systems to understand which stabilizer(s) are most optimal for nanoparticle catalyst synthesis and usage; particularly which systems have high catalytic activity and selectivity as well as long catalyst lifetimes. In agreement with Au nanoparticle stability results, PVP-stabilized PdAu nanoparticles were the most catalytically active due to improved nanoparticle stability, followed by nanoparticles stabilized by 1-methylimidazole, amine-functionalized IL, and the pure $BMIMPF_6$ IL.



## 1. Introduction

Due to their unique physiochemical properties such as high polarity, excellent thermal stability and negligible vapor pressures, room temperature ionic liquids (ILs) have provided an opportunity for chemists to studying reactions in an unique reaction media [1–3]. In the past few years ILs have also proven to be excellent solvents for the immobilization and stabilization of metal nanoparticles, thus providing an excellent media for quasi-homogeneous catalysis [4–19]. In particular, 1-butyl-3-methylimidazolium (BMIM)-based ILs have emerged as an effective media for the stabilization of nanoparticles [4–7,14,17–22]. Though there have been reports of the synthesis of gold and bimetallic nanoparticles in pure BMIM ILs without any additional stabilizers [17–19], a number of groups also reported the aggregation of gold nanoparticles in pure ILs [16,23,24]. To avoid these problems various secondary stabilizers such as poly(vinylpyrrolidone) (PVP) [25,26], task-specific ILs [27–34], and ionic liquid copolymers [35] have also been used for the synthesis of stable metal nanoparticles in ILs. In addition, our group has recently shown that low levels of 1-methylimidazole additives have dramatic effects on the stability of Au and bimetallic PdAu nanoparticles in imidazolium-based ionic liquids [36]. Thus while there have been a large number of different routes to synthesize and stabilize nanoparticle catalysts in ILs, to our knowledge there have been no comparative studies documenting the relative stability of nanoparticles using stabilizers in ILs or the effective relative activities and lifetimes of such nanoparticle/IL mixtures. This work is similar in nature to earlier pioneering work by El-Sayed and co-workers who showed that varying the type of stabilizer and the stabilizer/metal ratios had a profound effect on the activity and stability of Pt nanoparticles for Suzuki reactions in aqueous media, with the highest activities over short time periods often associated with particles which have the poorest long-term stabilities [37–39].

Deshmukh et al. were the first to show the formation of Pd nanoparticles in 1,3-di-*n*-butylimidazolium tetrafluoroborate ILs during Heck reactions [13]. Dupont and co-workers synthesized stable transition metal nanoparticles in pure imidazolium-based ILs without any secondary stabilizer, and the resulting nanoparticle catalysts were found to be active for a range of hydrogenation reactions [4–7,14,20]. Gomez and co-workers synthesized stable Pd nanoparticles stabilized by pure ILs and showed that the resulting nanoparticles had higher catalytic activity for a variety of Suzuki C–C cross-coupling and sequential reactions [40–42]. Several groups have indicated that the stabilization of nanoparticles in

* Corresponding author. Tel.: +1 306 966 2017; fax: +1 306 966 4730.
*E-mail address:* robert.scott@usask.ca (R.W.J. Scott).

1381-1169/$ – see front matter © 2010 Elsevier B.V. All rights reserved.
doi:10.1016/j.molcata.2010.06.022

ILs may be due to weak anion or cation interactions with nanoparticle surfaces [7,8,15,16], while others have noted that impurities such as halides and water could also have significant effects on nanoparticle stability [11,43]. Recently, we have shown that millimolar levels of 1-methylimidazole, a common starting material in imidazolium-based IL syntheses, can have dramatic effects on the stability of nanoparticles in ILs, which was a previously undocumented mode of stabilization [36]. In addition, we previously showed that highly stable Au, Pd and bimetallic PdAu nanoparticles can be synthesized by a simple phase-transfer method of PVP-stabilized nanoparticles from methanol to ILs, and that the resulting nanoparticles were catalytically active for a range of hydrogenation reactions [26].

Other groups have focused on the synthesis of task-specific ILs, which have specific functional groups attached to the imidazolium cations [30,31,44]. Such task-specific ILs have been shown to lead to enhanced nanoparticle stability and thus can be used to enhance catalytic activity of nanoparticles in ILs [27–30,32–34,45]. For example, Kim et al. have documented the synthesis of gold and platinum nanoparticles using thiol-functionalized ILs which bind to the nanoparticle surface and act as stabilizers [28]. Similarly, nitrile-functionalized ionic liquids have been used as a stabilizer to prevent agglomeration of Pd nanoparticles for the Stille coupling reaction between iodobenzene and tributylphenyltin, and were found to prevent catalyst deactivation [33]. Recently, Niu and co-workers synthesized stable Au nanoparticles using a functionalized IL, 1-(3-aminopropyl)-3-methylimidazolium bromide, and the resulting nanoparticles showed enhanced electrocatalytic activity and high stability [32]. Intrigued by this work, we chose to use a similar amine-functionalized task-specific IL as a stabilizer/surfactant dissolved in $BMIMPF_6$ for the synthesis of Au and bimetallic PdAu nanoparticles, and compare this stabilizer with other known methods for the stabilization of nanoparticles in ILs.

Given the numerous routes towards the synthesis of "stable" nanoparticles in ILs which exist in the literature, it can be very difficult to generalize as to which method(s) can lead to the optimal formation of stable, catalytically active nanoparticles. Thus, in order to compare a variety of stabilization methodologies, we synthesized pure Au and bimetallic PdAu nanoparticles in 1-butyl-3-methylimidazolium hexafluorophosphate ($BMIMPF_6$) ILs by four different methods. Nanoparticles were synthesized in $BMIMPF_6$ ILs by either direct synthesis or phase-transfer methods. In three different systems, PVP, 1-methylimidazole, and 1-(2′-aminoethyl)-3-methylimidazolium hexafluorophosphate ($aemimPF_6$) were added as secondary stabilizers while in the fourth system nanoparticles were directly synthesized in $BMIMPF_6$ ILs without any additional stabilizer. The long-term stability of pure Au nanoparticles in each of these systems was studied by UV–vis spectroscopy and transmission electron microscopy (TEM). Finally, in order to understand the effect that nanoparticle stability has on catalytic activity and catalyst lifetimes, bimetallic PdAu nanoparticles were synthesized by the four above-mentioned methods. Hydrogenation of two substrates, 1,3-cyclooctadiene and 3-buten-1-ol, was carried out to monitor their catalytic activity, and $^1H$ NMR spectroscopy was used to measure the activity in terms of turnover number (mol product/mol catalysts).

## 2. Experimental

### 2.1. Materials

1-Methylimidazole (99%) and 1-chlorobutane (99.5%) were purchased from Alfa and were distilled over KOH and $P_2O_5$, respectively, before use. Hexafluorophosphoric acid (*ca.* 65% solution in water), poly(vinylpyrrolidone) (M.W. 40,000), hydrogen tetrachloroaurate hydrate (99.9%), potassium tetrachloropalladate (99.99%), 3-buten-1-ol (98+%), and ethylenediamine (99%), and N-(2-bromoethyl)phthalimide (98+%) were purchased from Alfa and were used without further purification. 1,3-Cyclooctadiene (95%) and sodium borohydride powder (98%) were obtained from Aldrich and was used as obtained. Deuterated solvents were purchased from Cambridge Isotope Laboratories. 18 MΩ cm Milli-Q de-ionized water (Millipore, Bedford, MA) was used throughout.

### 2.2. Catalyst preparation

#### 2.2.1. Synthesis and purification of ILs

Synthesis of the 1-butyl-3-methylimidazolium hexafluorophosphate ($BMIMPF_6$) ILs was carried out under nitrogen and purified according to previously published procedures [26]. The purity of the $BMIMPF_6$ ILs was verified by $^1H$ NMR and UV–vis spectroscopy. In the final $BMIMPF_6$ ILs, the levels of 1-methylimidazole were below 0.5 mM through both careful NMR detection limit studies and colorimetric titrations with $Cu^{2+}$ salts while the water level was below 30 ppm by Karl–Fischer titration.

Synthesis of the functionalized IL, 1-(2′-aminoethyl)-3-methylimidazolium hexafluorophosphate ($aemimPF_6$) was carried out according to a previous literature procedure developed by Singer and co-workers, with minor modifications [46]. Briefly, N-(2-bromoethyl)phthalimide (113 mmol) was added to 100 ml freshly distilled toluene in a flask. Under $N_2$ atmosphere, freshly distilled 1-methylimidazole (125 mmol) was added to the flask, which was then heated at 70 °C for 72 h with constant stirring. After this step, the white crystalline powder, 1-(2′-phthalamidoethyl)-3-methylimidazolium bromide, was washed with 25 ml of cold toluene 3–4 times, dried after each washing step under vacuum, then stored in a desiccator under $P_2O_5$ for 2–3 days, and obtained in 38% yield. 1-(2′-Phthalamidoethyl)-3-methylimidazolium bromide (43 mmol) was dissolved in 100 ml of de-ionized water. A white precipitate was formed after the addition of $HPF_6$ (54 mmol) while cooling in an ice bath. The white precipitate, 1-(2′-phthalamidoethyl)-3-methylimidazolium hexafluorophosphate, was dried under vacuum for 6 h and then stored in a desiccator for 2 days, and obtained in 70% yield. Finally, $aemimPF_6$ was synthesized by gradual addition of ethylenediamine (200 mmol) over 15 min to a mixture of 1-(2′-phthalamidoethyl)-3-methylimidazolium hexafluorophosphate (25 mmol) in 200 ml of 1-butanol. The final solution was heated at 90 °C for 24 h under refluxing conditions. The reaction mixture was cooled to room temperature and washed with freshly distilled cold 1-butanol (distilled over $K_2CO_3$). The white solid, $aemimPF_6$, formed after 1-butanol was removed under vacuum for 8 h, and was then stored in a desiccator overnight. The yield of the final product was 50%. The purity of the product after each step was monitored by $^1H$ NMR.

#### 2.2.2. Synthesis of metallic and bimetallic nanoparticles

PVP, 1-methylimidazole stabilized, and "unstabilized" Au and bimetallic 3:1 PdAu nanoparticles were synthesized according to previously reported methods [26,36]. For all Au nanoparticle syntheses, the total gold concentration was 1.1 mM. PVP-stabilized nanoparticles were synthesized by a phase-transfer method from methanol to $BMIMPF_6$. "Unstabilized" nanoparticles were directly synthesized in pure $BMIMPF_6$ using $NaBH_4$ as a reducing agent, while nanoparticles stabilized by 1-methylimidazole were made similarly except in the presence of 1 mM 1-methylimidazole additives [36].

Au nanoparticles using $aemimPF_6$ as a stabilizer were synthesized by a phase-transfer method. A 10 mM solution of $aemimPF_6$ was dissolved in 10 ml water in a round-bottomed flask. In another flask, 1.0 ml of 10 mM $HAuCl_4$ in $BMIMPF_6$ was added to 8.0 ml

of pure $BMIMPF_6$. The mixture was stirred for 15 min, followed by the addition of 1.0 ml of a 0.10 M $NaBH_4$ solution in $BMIMPF_6$ prepared 12 h before use. The total solution volume was 10.0 ml. The immediate formation of a deep red solution occurred upon addition of $NaBH_4$ to the solution, indicating the formation of Au nanoparticles. Then, the aqueous solution of $aemimPF_6$ was added with vigorous stirring to the Au nanoparticles in $BMIMPF_6$, followed by the removal of water under vacuum. Bimetallic 3:1 PdAu nanoparticles were also made directly in $BMIMPF_6$ using $aemimPF_6$ as a stabilizer. First, 9.38 ml of a 107 mM solution of $aemimPF_6$ in $BMIMPF_6$ was prepared. This solution was stirred for 15 min, followed by the addition of 0.165 ml of 10 mM $K_2PdCl_4$ in $BMIMPF_6$ and 0.055 ml of 10 mM $HAuCl_4$ in $BMIMPF_6$. The mixture was stirred for 15 min, followed by the addition of 0.40 ml of 0.10 M $NaBH_4$ in $BMIMPF_6$ prepared 12 h before use. The total solution volume was 10.0 ml.

### 2.3. Catalytic reactions

Hydrogenation reactions were carried out in a three-necked round-bottom flask at 40 °C. One end of the flask was connected to the $H_2$ gas source, the other end was attached to a differential pressure gauge (Model 407910, Extech Instruments Corp.) and the central portion was closed with a rubber septum. First, 10 ml of the catalyst solution was placed in the flask, followed by purging the system with continuous $H_2$ flow. Next, the 1,3-cyclooctadiene and/or 3-buten-1-ol substrate was added by syringe under vigorous stirring conditions (at 1080 rpm), followed by measurement of samples by $^1H$ NMR. The hydrogen pressure used for all reactions was 1.0 atm, and the substrate:catalyst ratios were 400:1 for the 1,3-cyclooctadiene substrate and 15904:1 for 3-buten-1-ol. The turnover number (TON, mol product/mol catalyst) and selectivities for product distributions were determined by $^1H$ NMR. After 1 and 17 h intervals, 1 ml of the solution was placed in a vial and then $CDCl_3$ was added. The vial was shaken to transfer the products into the $CDCl_3$ phase which was then removed and used for NMR analysis. All conditions (temperature, stirring speed, *etc.*) were kept constant throughout all hydrogenation reactions. For 1,3-cyclooctadiene, the reaction was also followed by measurement of the $H_2$ uptake through differential pressure measurements every 10 s. This, in turn allowed calculating the moles of hydrogen consumed, which by NMR measurements was found to correlate within 3% to the moles of cyclooctene product. This allowed for real-time measurements of the effective turnover number of the catalyst system.

### 2.4. Characterization

UV–vis spectra were obtained using a Varian Cary 50 Bio UV–vis spectrophotometer with a scan range of 300–900 nm with an optical path length of 1.0 cm. The $^1H$ NMR spectra were obtained using a Brüker 500 MHz Advance NMR spectrometer. $^1H$ NMR chemical shifts were referenced to the residual protons of the deuterated solvent. TEM micrographs were obtained with a Philips 410 microscope operating at 100 kV. To prepare samples for TEM, a drop of a methanol/IL mixture containing the nanoparticles was placed on a holey-carbon-coated Cu TEM grid (200 mesh) which had been preoxidized by air plasma treatment, followed by evaporation of the methanol. Typically the size of 150 nanoparticles was measured for each sample from several different locations on the grid.

## 3. Results and discussion

Unraveling the possible modes of stabilization of nanoparticles in ionic liquids is a considerable challenge, particularly given the unique nature of the medium. In order to most effectively probe nanoparticle aggregation in solution, Au nanoparticles were chosen as the first system to investigate. The dipole–dipole interactions between plasmon bands of aggregated gold nanoparticles is manifested as a shift of the plasmon band wavelength, and thus a change in colour of the solution from red to purple, which can be easily monitored by UV–vis spectroscopy [47]. The initial system studied is the formation of gold nanoparticles in pure $BMIMPF_6$ ionic liquids, *i.e.* "unstabilized" Au nanoparticles. As noted in Section 1, a number of groups, including ours, have shown that Au nanoparticles are prone to aggregation in ionic liquids over a time period ranging from minutes to weeks [16,23,24,36]. It should be noted that extremely clean ILs need to be used in order to compile reproducible results in such systems; in our case, the BMIMCl precursors are recrystallized at least four times from acetone, and $Cl^-$ impurities from the final $BMIMPF_6$ ILs are removed via multiple washes with de-ionized water until no AgCl precipitates form in the washings upon addition of $AgNO_3$. The final $BMIMPF_6$ ionic liquids are then dried overnight under vacuum, resulting in water levels below 30 ppm by Karl–Fischer titrations. Karl–Fischer titrations have been used by a large number of other groups for the determination of water levels in ILs [3,48]; however, it should be noted that such titrations may lead to systematic underestimation of water content as water tightly bound to anions and/or cations or trapped in the IL structure and may be inaccessible for titration [49]. Finally, detailed NMR detection limit studies have shown that 1-methylimidazole impurities are below 0.5 mM in the clean ILs.

Fig. 1A shows the UV–vis spectra over time of Au nanoparticles synthesized in pure $BMIMPF_6$. A decrease in the intensity of the plasmon band at 530 nm along with an increase in the high-wavelength region of the absorption spectra over 17 h is seen, which is indicative of particle aggregation in solution [23,50]. Indeed the nanoparticles precipitated out from the solution after several weeks. It should be noted that while the particles are prone to aggregation and precipitation, the particles do not grow in size as a consequence of aggregation; TEM images indicate the final precipitates are composed of particles of similar size as the originally synthesized nanoparticles (see below). We are still unsure as to exactly what the dominant mode of stabilization of such nanoparticles in pure $BMIMPF_6$ solutions, particularly compared to conventional solvents in which nanoparticle aggregation and precipitation is nearly instantaneous in the absence of external stabilizers. Others have indicated that weak anion and/or cation interactions with the nanoparticles can lead to steric stabilization of the nanoparticles [7,8,15,16], but it is unlikely that this could lead to conventional double-layer stabilization given the high polarity of the IL media. Another factor is the possibility of impurities in the IL promoting nanoparticle stabilization; control reactions have indicated that the addition of chloride and/or bromide salts do not enhance nanoparticle stability, but 1-methylimidazole additives do (see below) [36]. Thus it is possible that 1-methylimidiazole impurities below the NMR detection limit could be contributing to partial nanoparticle stability. Finally, one major factor in the slow aggregation and precipitation of the nanoparticles is the high viscosity of ILs, which is typically two orders of magnitude greater than conventional solvents ($BMIMPF_6$ has a viscosity of *ca.* 450 cP) [3]. The high viscosity of $BMIMPF_6$ would result in a dramatically reduced number of nanoparticle–nanoparticle collisions in ILs due to Brownian motion of the particles. However, if stability were simply a consequence of the nanoparticle–nanoparticle collision frequency, then stirring Au nanoparticle/$BMIMPF_6$ suspensions should lead to increased rates of aggregation; however this is not observed experimentally. Instead, stirring of Au nanoparticle/$BMIMPF_6$ suspensions tends to break apart aggregates, suggesting the force(s) driving nanoparticle aggregation are quite weak in $BMIMPF_6$.

Fig. 1B shows the UV–vis spectra of Au nanoparticles synthesized in the presence of PVP additives. Note that in the case

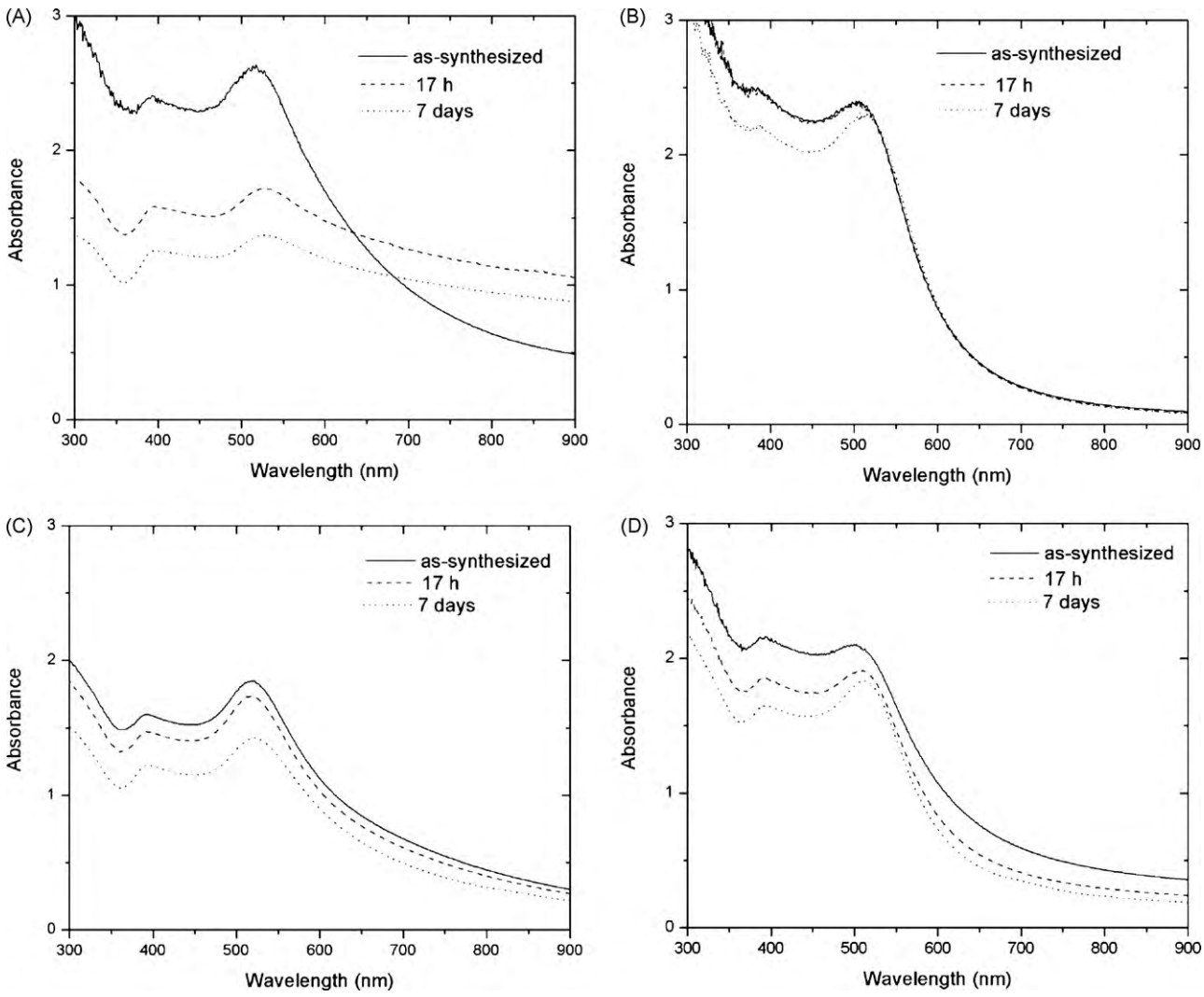


**Fig. 1.** UV–vis absorption spectra of Au nanoparticles over time in (A) pure $BMIMPF_6$, (B) $BMIMPF_6$ with 1.39 mM PVP additive, (C) $BMIMPF_6$ with 1 mM 1-methylimidazole additive, and (D) $BMIMPF_6$ with 10 mM $aemimPF_6$ additive.

for PVP-stabilized nanoparticles, the particles were first synthesized in MeOH and then transferred over to the $BMIMPF_6$ IL via removal of the methanol under vacuum, due to the difficulty in directly dissolving PVP in the IL. As can be noted in Fig. 1B, PVP-stabilized Au nanoparticles show no significant aggregation in the UV–vis spectra observed over a period of 1 week. Fig. 1C and D shows the representative UV–vis spectra of 1-methylimidazole and $aemimPF_6$-stabilized nanoparticles. The drop in intensity of the UV–vis spectra for these systems is due to a fraction of Au nanoparticles adhering to the sides of the glass reaction flask over time, which was not observed for the PVP system; however minimal aggregation was observed compared to the "unstabilized" Au nanoparticles, which have a rising baseline over time (Fig. 1A). Best results for $aemimPF_6$-stabilized particles were obtained for particles originally synthesized in pure $BMIMPF_6$ followed by addition of the $aemimPF_6$ stabilizer; attempts to synthesize particles directly in the presence of the stabilizer led to poorly stabilized particles, likely due to the (surprisingly) low solubility of the $aemimPF_6$ phase in $BMIMPF_6$. Also, attempts to synthesize $aemimPF_6$-stabilized Au nanoparticles in water or alcohol solvents followed by phase transfer to the IL phase were unsuccessful due to the fast precipitation of the particles from the aqueous or alcohol phases. Wang et al. previously noted that aemimBr stabilized Au nanoparticles were quite stable in water; we believe that the major stabilizer in the latter case is the $Br^-$ anion [32], which has been observed previously for both TOAB and CTAB stabilized Au nanoparticles [51,52].

Of all the four systems, the PVP-stabilized Au nanoparticles in $BMIMPF_6$ are definitely the most stable, with no changes seen via UV–vis for periods of several months. In order to fully study the nanoparticle stability, TEM images of the nanoparticles as-synthesized and after several weeks were also collected. It should be noted that TEM evidence alone should not be used as a proof of aggregation (or lack thereof) as artifacts can occur upon casting nanoparticles onto TEM grids. Typically for TEM grid preparation, solution phase nanoparticles are cast onto carbon-coated grids followed by solvent evaporation, which is untenable in the presence of pure ILs which have negligible volatility. In order to effectively make TEM samples, IL/nanoparticle mixtures were diluted in methanol and cast onto TEM grids, followed by methanol evaporation, such that the IL solvent is still present under TEM conditions. Fig. 2 shows the TEM images of Au nanoparticles among the four stabilizing systems. In the absence of any stabilizers aggregation of Au nanoparticles was seen even at short periods of time, with an average particle size of $4.8 \pm 0.7$ nm. It should be noted that even after 2 weeks, only a small change in the size of the nanoparticles is seen, with the particles growing to $5.3 \pm 0.8$ nm (see Fig. 3A). In the presence of PVP, the average Au nanoparticle size is much smaller, $3.3 \pm 0.6$ nm, with minimal aggregation seen for the as-synthesized

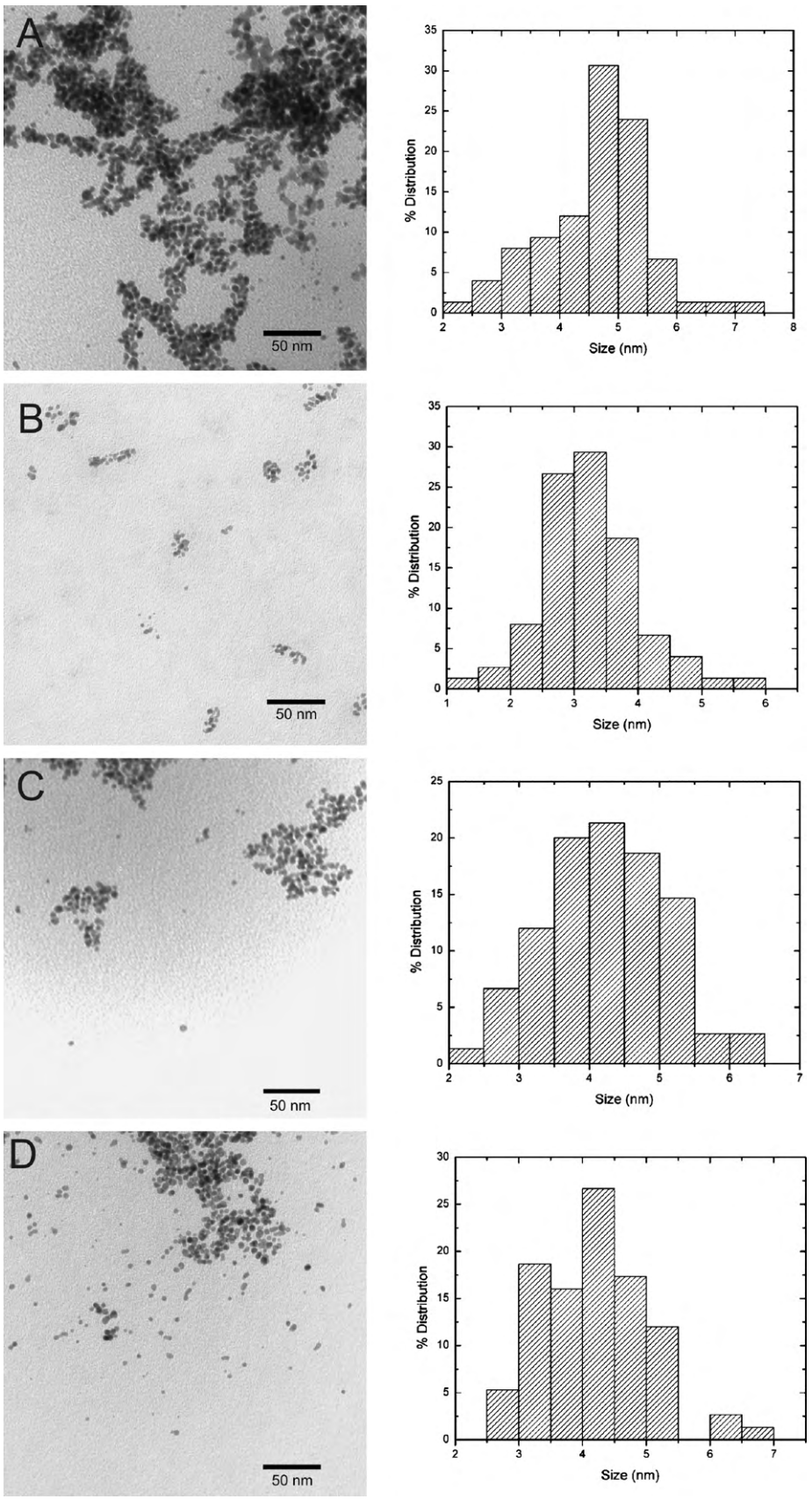


**Fig. 2.** TEM images and particle size histograms of as-synthesized Au nanoparticles in (A) pure $BMIMPF_6$, (B) $BMIMPF_6$ with 1.39 mM PVP additive, (C) $BMIMPF_6$ with 1 mM 1-methylimidazole additive, and (D) $BMIMPF_6$ with 10 mM $aemimPF_6$ additive.

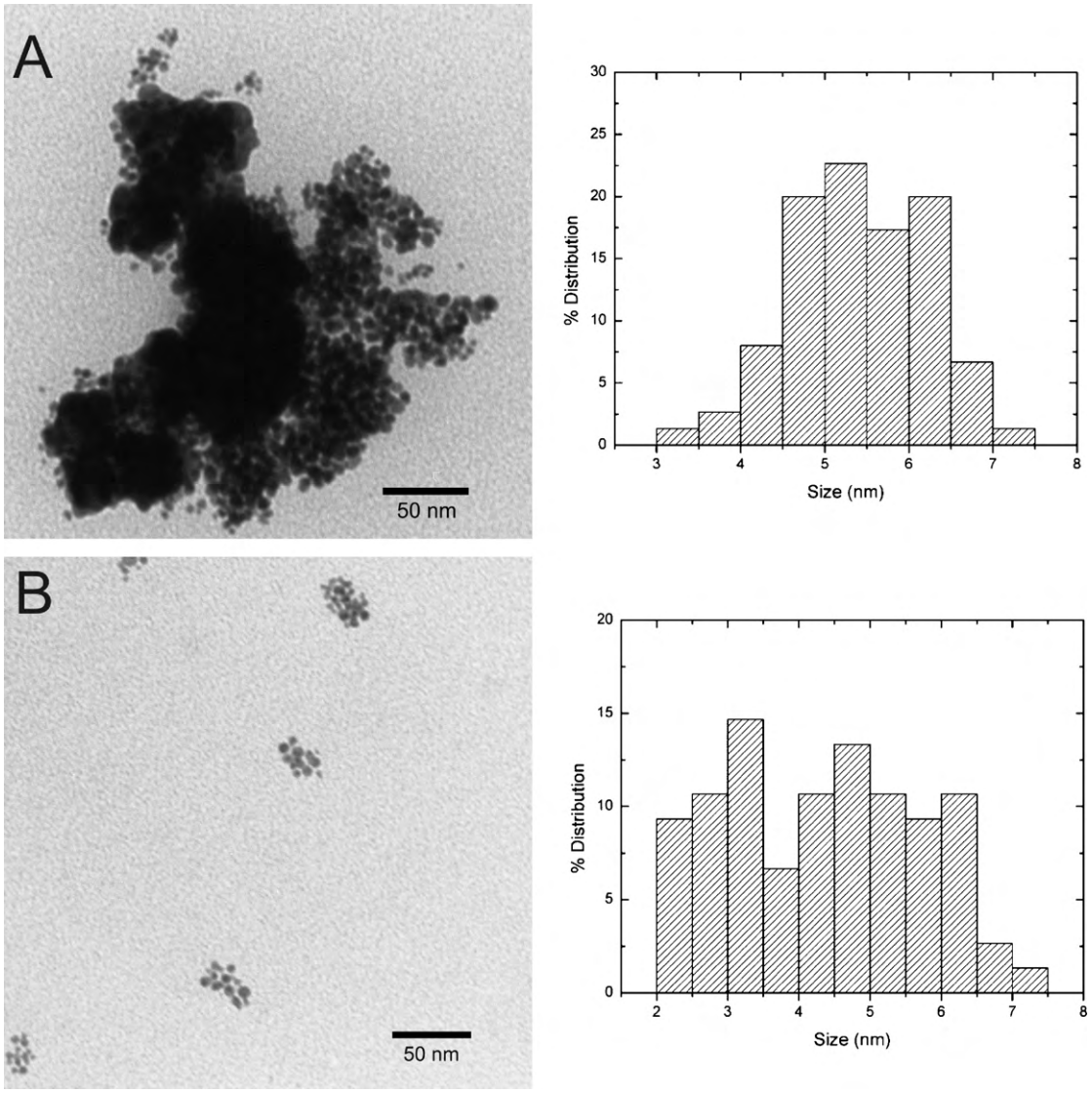


**Fig. 3.** TEM images of Au nanoparticles after two weeks in (A) pure $BMIMPF_6$ and (B) $BMIMPF_6$ with 1.39 mM PVP additive.

samples and slight particle size growth to $4.3 \pm 1.4$ nm after 2 weeks with an apparent bimodal distribution developing (Figs. 2B and 3B). We are not certain why this particle size growth/broadening distribution is occurring, but it may be indicative of Ostwald ripening processes at work over long time scales. In the presence of 1-methylimidazole, minimal particle aggregation with an average particle size of $4.2 \pm 0.7$ nm was seen, while aemim$PF_6$-stabilized particles were found to be $4.3 \pm 0.8$ nm with moderate aggregation.

Finally, before moving on to discuss the catalytic activity of nanoparticles in these systems, several remarks on the generality of the stability results are warranted; in particular, how changing the cation and/or anion of the IL can affect nanoparticle stability and whether borohydride and borohydride oxidation products are affecting particle stability. $BMIMPF_6$ ILs were chosen as the IL of choice due to the copious literature that exists on nanoparticle stability in $BMIMPF_6$. We have not examined cation changes beyond the generation of aemim$PF_6$ stabilizers, however, attempts to grow Au nanoparticles in pure BMIMOTf ILs have been attempted; in the absence of stabilizer, fast precipitation (~10–20 min) of Au nanoparticles is seen for particles stabilized in pure BMIMOTf, and we have previously noted that much larger amounts of 1-methylimidazole (*ca.* 100 mM) are necessary for stabilization of Au nanoparticles in BMIMOTf [36]. This result suggests that weak anion interactions with Au nanoparticles may be partially responsible for the underlying stability of particles in $BMIMPF_6$. Also, we note that no attempts were made to remove sodium borohydride oxidation products after the synthesis of the nanoparticles; however, control examples of PVP-stabilized Au particles which were synthesized in water and dialyzed before phase exchange into $BMIMPF_6$ showed similar stabilities to those mentioned above.

## 4. Nanoparticle catalysis

Having studied the stability of Au nanoparticles in $BMIMPF_6$ by the four different stabilization strategies above, we wished to further investigate whether these findings would influence the catalyst lifetime of nanoparticles in $BMIMPF_6$ as well. In order to do this, we chose to investigate bimetallic 3:1 PdAu nanoparticles as catalysts for the hydrogenation of 1,3-cyclooctadiene and 3-buten-1-ol. We have previously shown that PVP-stabilized PdAu bimetallic nanoparticles in $BMIMPF_6$ are active hydrogenation catalysts for a range of substrates, and that co-reduced 3:1 PdAu nanoparticles had the highest activity [26]. In addition, we later showed that bimetallic 3:1 PdAu nanoparticles stabilized

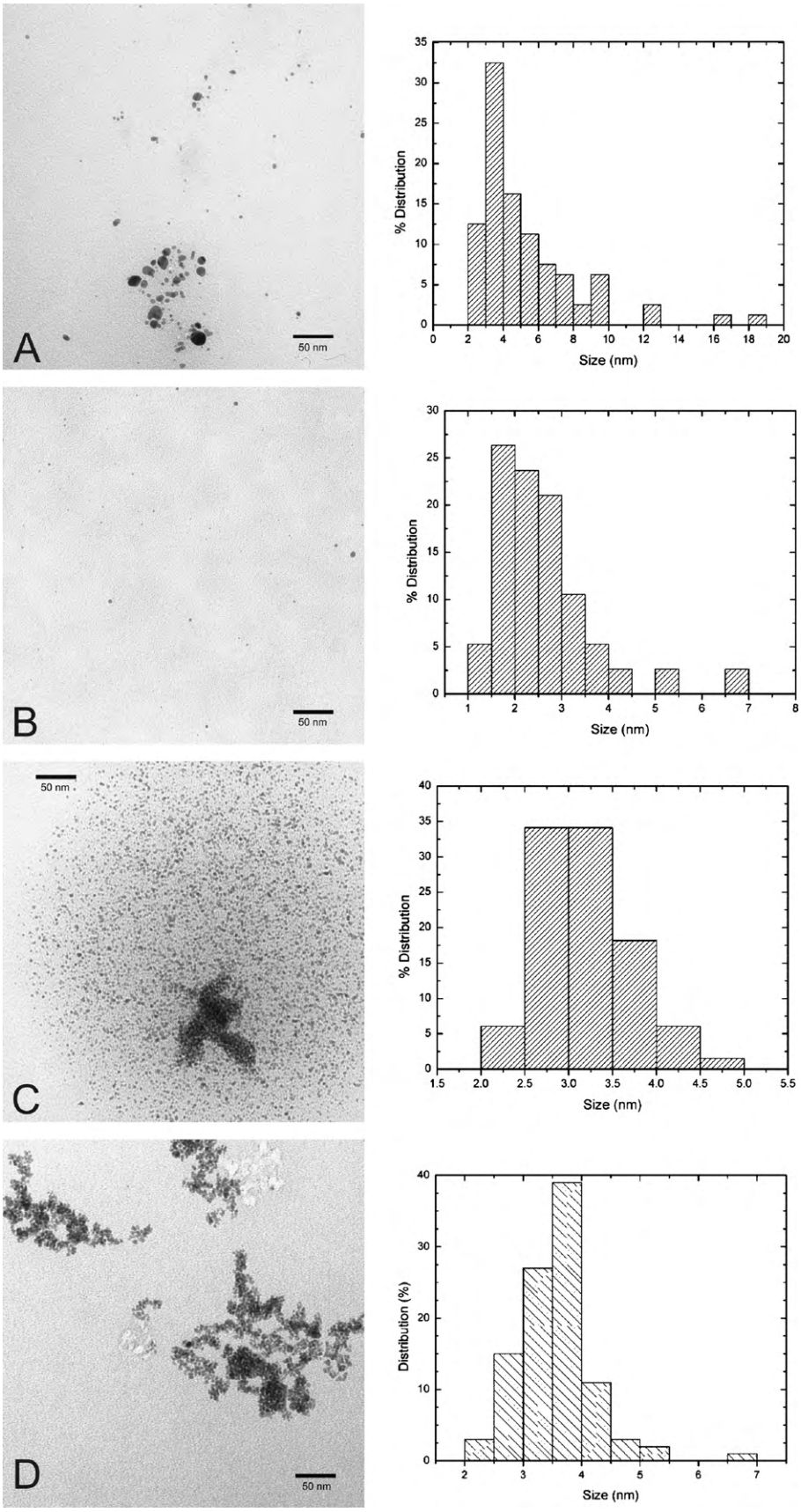


**Fig. 4.** TEM images and particle size histograms of as-synthesized 3:1 PdAu nanoparticles in (A) pure $BMIMPF_6$, (B) $BMIMPF_6$ with 1.39 mM PVP additive, (C) $BMIMPF_6$ with 1 mM 1-methylimidazole additive, and (D) $BMIMPF_6$ with 10 mM $aemimPF_6$ additive.

by 1-methylimidazole in $BMIMPF_6$ were active catalysts for the hydrogenation of allyl alcohol [36]. However, the design of stabilized nanoparticles with long catalyst lifetimes (and therefore total turnover numbers) remains an important challenge, particularly if "greener" IL solvents are to replace conventional solvents and/or heterogeneous catalysts.

Bimetallic 3:1 PdAu nanoparticles were synthesized following similar procedures for the pure Au nanoparticles; PVP-stabilized particles were synthesized in methanol and transferred to the IL phase, while other samples were synthesized directly in neat $BMIMPF_6$ IL or in the IL with 1-methylimidazole or $aemimPF_6$ additives present. Fig. 4 shows representative TEM images of the bimetallic nanoparticles produced by each method. TEM analysis indicates that the PVP-stabilized particles had the smallest average particle size of $2.6 \pm 1.1$ nm, with no particle aggregation seen by TEM, as seen in Fig. 4. Particles synthesized in the presence of 1-methylimidazole had an average particle size of $3.2 \pm 0.6$ nm, while $aemimPF_6$-stabilized nanoparticles had an average particle size of $3.6 \pm 0.7$ nm and nanoparticles synthesized in the neat $BMIMPF_6$ IL had much greater average particle sizes ($5.3 \pm 3.0$ nm) and polydispersity than any of the stabilized samples. These findings are consistent with the earlier Au nanoparticle results; in the absence of any secondary stabilizer, significantly larger particles are seen, while PVP stabilizers yield particles with the smallest average particle sizes. UV–vis spectra for all the particles showed an exponentially decaying absorption towards higher wavelengths and the complete absence of any Au plasmon bands, which is consistent with the formation of particles with PdAu alloy structures [53]. Previous work in our group has shown that PVP-stabilized PdAu nanoparticles synthesized via borohydride reduction of mixtures of their salts have near-alloy structures via single-particle energy-dispersive spectroscopy (EDS) and extended X-ray absorption fine structure (EXAFS) measurements [54]. Unfortunately, we were not able to collect accurate single-particle EDS measurements for particles synthesized directly in the ionic liquid, due to sample "burning" effects caused by the ionic liquid present on the TEM grids.

We investigated the catalytic activity of 3:1 PdAu nanoparticles towards the hydrogenation of cylcooctadiene and 3-buten-1-ol using each of the four stabilizer systems as previously examined in the pure Au system. Fig. 5A shows the plot of the effective turnover number vs. time for the partial hydrogenation of cylcooctadiene for each of the four systems. We have previously shown that 3:1 PdAu catalysts are extremely selective for the partial hydrogenation to cyclooctene [26], and NMR results confirmed that the major product of this reaction was cyclooctene with 98–99% selectivities for all of the systems studied. Effective turnover numbers were collected in real-time for all samples by monitoring the decrease in partial pressure of $H_2$ during the reaction; NMR results indicated that the $H_2$ consumed correlated nearly exactly with the amount of product formed (±3%). As can be seen in Fig. 5A, the PVP-stabilized PdAu nanoparticles initially showed the lowest activity, but retained their activity during the course of the reaction, while the particles synthesized in the absence of any additives showed a dramatic drop off in activity in the first 10 min of the reaction and showed a visible precipitate after 1 h. Particles stabilized by 1-methylimidazole and $aemimPF_6$ had intermediate activities for the hydrogenation and did not show any visible precipitation. Fig. 5B shows the similar plot in which the effective turnover number is normalized for the moles of surface metal on the particles; this was done to compensate for the dramatically different particle sizes as seen by TEM. We note that the unstabilized particles have significantly initial activities for this reaction; these results suggest that the PVP, 1-methylimidazole, and $aemimPF_6$ stabilizers do partially passivate the particle surface during the hydrogenation reaction. Attempts were made to examine the effect of PVP loading on the catalytic activity of the particles, however, it was found

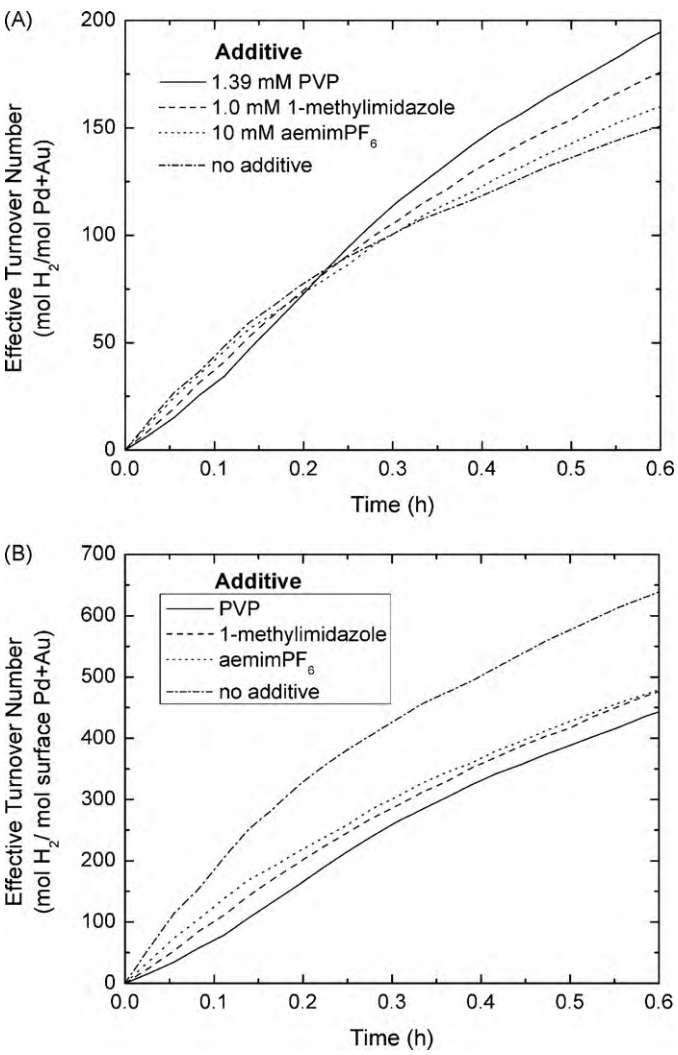


**Fig. 5.** (A) Effective turnover number (moles $H_2$/moles Pd + Au) vs. time plot and (B) plot of surface turnover number (moles $H_2$/moles surface Pd + Au) vs. time plot for hydrogenation of 1,3-cyclooctadiene in the presence of additives. Substrate:catalyst ratio = 400:1.

that at lower PVP loadings of 0.7 mM and below the particles were unstable to aggregation upon phase exchange, while at higher PVP loadings of 2.8 mM and above the IL was so viscous that negligible activity was observed due to mass transfer limitations.

3-Buten-1-ol was used as a second substrate to probe the long-term activity and stability of the PdAu nanoparticle catalysts. Allylic alcohols such as allyl alcohol and 2-buten-1-ol can also form extensive amounts of aldehyde products under hydrogenation conditions [55]. The observed reaction products for the hydrogenation and/or isomerization(s) of 3-buten-1-ol are shown in Scheme 1. Initially, PVP-stabilized PdAu nanoparticles were used to optimize the catalyst conditions. While high activities could be observed at low catalyst concentrations, attempts to increase the substrate:catalyst ratio and thus the theoretical maximum turnover numbers in these reactions by lowering the amount of catalyst were unsuccessful, as extremely low yields were seen as the catalyst concentration was lowered. It was found that the optimal conditions for maximizing the turnover number of the desired product/lifetime of the catalysts was for 0.22 mM 3:1 PdAu catalysts with a substrate:catalyst ratio of approximately 16,000:1; 100% substrate conversion with and a 1-butanol-specific TON of over 10,000 was obtained. The selectivity towards the hydrogenation product was only 68%, as the other minor products in this reaction were the isomerization product,

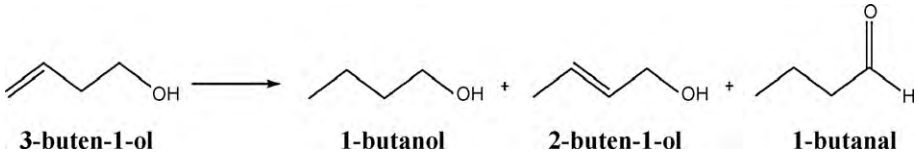


**Scheme 1.** Products detected during the hydrogenation of 3-buten-1-ol.

2-buten-1-ol (22%), and a minor amount of 1-butanal (10%), a double isomerization/tautomerization product [56]. The PVP-stabilized PdAu nanoparticles were stable over the reaction period of time and no precipitation was observed during the reaction. Similar results were seen for PVP-stabilized PdAu nanoparticles synthesized and dialyzed in water prior to phase exchange into $BMIMPF_6$; thus the presence of borohydride oxidation products does not have any significant effect on the catalytic activity of the particles. We note that pure Pd nanoparticles typically show selectivities of *ca.* 55% for this reaction with lower activities; thus a mild enhancement of selectivity for the PdAu nanoparticles is seen for this substrate.

These optimized conditions were used to compare each of the four stabilizing systems, and the results can be found in Table 1. The PVP-stabilized PdAu nanoparticles had the highest catalytic activity of all the systems studied, while particles synthesized in pure $BMIMPF_6$ showed the lowest conversions. Indeed, "unstabilized" PdAu nanoparticles were found to precipitate out of the IL solution within a period of several hours; however, it is interesting to note that while the catalytic activity of the particles is much lower, they still remained catalytically active even after precipitation. Because of this aggregation over time, we make no attempt to normalize activities to account for different particle sizes. Interestingly, the isomerization product 2-buten-1-ol was observed as a major impurity in all the catalytic reactions; the lower amounts of 2-buten-1-ol seen for the PVP-stabilized nanoparticles may be due to the secondary hydrogenation of this substrate to give 1-butanol, although catalytic data suggests the PdAu catalysts are less active for the hydrogenation of 2-buten-1-ol compared to the original substrate 3-buten-1-ol. Two catalytic tests were attempted with the methylimidazole stabilized PdAu nanoparticles, at 1-methylimdiazole concentrations of 1 and 100 mM, respectively. Interestingly, much higher TONs were seen for particles in the presence of 1 mM 1-methylimidazole, suggesting that passivation of catalytic sites is occurring at higher 1-methylimidazole concentrations. Such passivation was not previously seen at short time periods for 1-methylimidazole stabilized PdAu nanoparticles [36].

Finally, the catalytic activity of the $aemimPF_6$-functionalized PdAu nanoparticles is intermediate between that of PVP and the absence of stabilizer, which is in agreement with stability results using Au nanoparticles. Initially, PdAu nanoparticles were directly synthesized in $BMIMPF_6$ ILs in the presence of 100 mM of the $aemimPF_6$ stabilizer. Alternatively, we tried to synthesize $aemimPF_6$-stabilized PdAu nanoparticles by a phase-transfer method in which PdAu nanoparticles were directly synthesized in pure $BMIMPF_6$ ILs, followed by addition of 10 mM $aemimPF_6$. The catalytic activity of these nanoparticle catalysts was found to be much lower (25% conversion at 17 h), possibly due to the lower concentration of stabilizer. Low $aemimPF_6$ solubility in the $BMIMPF_6$ ILs limited attempts to increase the concentration of $aemimPF_6$ beyond 100 mM. One interesting factor to note in catalytic data for the $aemimPF_6$-stabilized particles is the complete absence of 1-butanal formation; the possible reason(s) for this selectivity change are still unknown, but may involve the in situ formation of 1-butanal and the subsequent reaction with the primary amine group of $aemimPF_6$ to form imines.

The catalytic results show a similar trend in long-term activity as seen in the stability studies with pure Au nanoparticles; PVP-stabilized nanoparticles were the most active system, followed by 1-methylimidazole, $aemimPF_6$, and "unstabilized" PdAu nanoparticles, respectively. The increased activity of the PVP-stabilized PdAu nanoparticles compared to 1-methylimidazole and $aemimPF_6$-stabilized particles may be partially due to the slightly lower nanoparticle sizes of these particles compared to the other systems; similar average nanoparticle sizes were seen by TEM for both the Au and PdAu nanoparticle syntheses. PdAu nanoparticles synthesized in pure $BMIMPF_6$ ILs had particularly low long-term catalytic activities due to their fast aggregation and precipitation; however, it should be noted that unlike other solvent systems, the aggregated PdAu nanoparticles in $BMIMPF_6$ still retain some catalytic activity even after precipitation. This is likely due to the fact that while aggregation of the particles is seen during the catalytic reactions, no significant change in the average particle size in the aggregates was seen. Finally, we note that PVP-stabilized nanoparticles can easily

**Table 1**
Hydrogenation of 3-buten-1-ol by four different stabilizers in $BMIMPF_6$ ILs.

| Stabilizer | % conversion | 1-Butanol-TON | Selectivity | |
|---|---|---|---|---|
| PVP | 100 | 10815 | 1-Butanol | 68% |
| | | | 2-Buten-1-ol | 22% |
| | | | 1-Butanal | 10% |
| 1-Methylimidazole (1 mM) | 83.5 | 5805 | 1-Butanol | 40% |
| | | | 2-Buten-1-ol | 50% |
| | | | 1-Butanal | 10% |
| 1-Methylimidazole (100 mM) | 32.5 | 2016 | 1-Butanol | 39% |
| | | | 2-Buten-1-ol | 53% |
| | | | 1-Butanal | 8% |
| $aemimPF_6$ (100 mM) | 60.6 | 5590 | 1-Butanol | 58% |
| | | | 2-Buten-1-ol | 42% |
| | | | 1-Butanal | 0% |
| Pure $BMIMPF_6$ | 39.5 | 1822 | 1-Butanol | 29% |
| | | | 2-Buten-1-ol | 62% |
| | | | 1-Butanal | 9% |

Conditions: 40 °C, 0.22 mM [Au + Pd], substrate:catalyst ratio = 15,904:1, time = 17 h.

be recovered and used for subsequent catalytic reactions [26], while the 1-methylimidazole and aemim$PF_6$-stabilized nanoparticles did not retain their activity over multiple catalytic runs.

## 5. Conclusions

We have described four stabilization protocols for nanoparticle stabilization in BMIM$PF_6$ ILs, and have shown that nanoparticle stability and thus catalytic activity of nanoparticles is dependent on the overall stability of the nanoparticles towards aggregation. The four different stabilization methods in BMIM$PF_6$ which were used include the synthesis of nanoparticles in pure ILs, and the addition of secondary PVP, 1-methylimidazole, and aemim$PF_6$ stabilizers. The activity and lifetimes of 3:1 PdAu nanoparticle catalysts synthesized by these four methods were measured by hydrogenation of 1,3-cyclooctadiene and 3-buten-1-ol substrates. PVP-stabilized nanoparticles were found to be the most stable, and had the highest catalytic activity and longer lifetimes than catalysts prepared by the other stabilization routes. As there are a large number of routes towards the development of size-, shape-, and composition-selected nanoparticle syntheses using poly(vinylpyrrolidone) polymers, the inherent stability of these particles in IL solvents suggests that a wide range of particles can be made in more conventional aqueous and alcoholic solvents, transferred to ILs, and used for subsequent catalytic reactions.

## Acknowledgements

The authors would like to acknowledge financial assistance from the National Sciences and Engineering Research Council of Canada (NSERC), and Prof. Ian Burgess for helpful discussions.

## References

[1] P. Wasserscheid, W. Keim, Angew. Chem. Int. Ed. 39 (2000) 3772–3789.
[2] T. Welton, Chem. Rev. 99 (1999) 2071–2083.
[3] J.G. Huddleston, A.E. Visser, W.M. Reichert, H.D. Willauer, G.A. Broker, R.D. Rogers, Green Chem. 3 (2001) 156–164.
[4] J. Dupont, G.S. Fonseca, A.P. Umpierre, P.F.P. Fichtner, S.R. Teixeira, J. Am. Chem. Soc. 124 (2002) 4228–4229.
[5] G.S. Fonseca, A.P. Umpierre, P.F.P. Fichtner, S.R. Teixeira, J. Dupont, Chem. Eur. J. 9 (2003) 3263–3269.
[6] C.W. Scheeren, G. Machado, J. Dupont, P.F.P. Fichtner, S.R. Texeira, Inorg. Chem. 42 (2003) 4738–4742.
[7] P. Migowski, J. Dupont, Chem. Eur. J. 13 (2007) 32–39.
[8] M. Antonietti, D. Kuang, B. Smarsly, Y. Zhou, Angew. Chem. Int. Ed. 43 (2004) 4988–4992.
[9] E. Redel, R. Thomann, C. Janiak, Inorg. Chem. 47 (2008) 14–16.
[10] E. Redel, R. Thomann, C. Janiak, Chem. Commun. (2008) 1789–1791.
[11] V.I. Pârvulescu, C. Hardacre, Chem. Rev. 107 (2007) 2615–2665.
[12] J. Huang, T. Jiang, B.X. Han, H.X. Gao, Y.H. Chang, G.Y. Zhao, W.Z. Wu, Chem. Commun. (2003) 1654–1655.
[13] R.R. Deshmukh, R. Rajagopal, K.V. Srinivasan, Chem. Commun. (2001) 1544–1545.
[14] C.W. Scheeren, G. Machado, S.R. Teixeira, J. Morais, J.B. Domingos, J. Dupont, J. Phys. Chem. B 110 (2006) 13011–13020.
[15] D. Astruc, F. Lu, J.R. Aranzaes, Angew. Chem. Int. Ed. 44 (2005) 7852–7872.
[16] H.S. Schrekker, M.A. Gelesky, M.P. Stracke, C.M.L. Schrekker, G. Machado, S.R. Teixeira, J.C. Rubim, J. Dupont, J. Colloid Interface Sci. 316 (2007) 189–195.
[17] K.-S. Kim, S. Choi, J.-H. Cha, S.-H. Yeon, H. Lee, J. Mater. Chem. 16 (2006) 1315–1317.
[18] J. Zhu, Y. Shen, A. Xie, L. Qiu, Q. Zhang, S. Zhang, J. Phys. Chem. C 111 (2007) 7629–7633.
[19] K.-I. Okazaki, T. Kiyama, K. Hirahara, N. Tanaka, S. Kuwabata, T. Torimoto, Chem. Commun. (2008) 691–693.
[20] A.P. Umpierre, G. Machado, G.H. Fecher, J. Morais, J. Dupont, Adv. Synth. Catal. 347 (2005) 1404–1412.
[21] E.T. Silveira, A.P. Umpierre, L.M. Rossi, G. Machado, J. Morais, G.V. Soares, I.L.R. Baumvol, S.R. Teixeira, P.F.P. Fichtner, J. Dupont, Chem. Eur. J. 10 (2004) 3734–3740.
[22] M.A. Gelesky, A.P. Umpierre, G. Machado, R.R.B. Correia, W.C. Magno, J. Morais, G. Ebeling, J. Dupont, J. Am. Chem. Soc. 127 (2005) 4588–4589.
[23] G.T. Wei, Z.S. Yang, C.Y. Lee, H.Y. Yang, C.R.C. Wang, J. Am. Chem. Soc. 126 (2004) 5036–5037.
[24] Y. Wang, H. Yang, Chem. Commun. (2006) 2545–2547.
[25] X. Mu, D.G. Evans, Y. Kou, Catal. Lett. 97 (2004) 151–154.
[26] P. Dash, N.A. Dehm, R.W.J. Scott, J. Mol. Catal. A: Chem. 286 (2008) 114–119.
[27] R. Tatumi, H. Fujihara, Chem. Commun. (2005) 83–85.
[28] K.-S. Kim, D. Demberelnyamba, H. Lee, Langmuir 20 (2004) 556–560.
[29] D. Zhao, Z. Fei, T. Geldbach, R. Scopelliti, P. Dyson, J. Am. Chem. Soc. 126 (2004) 15876–15882.
[30] A.E. Visser, R.P. Swatloski, W.M. Reichert, R. Mayton, S. Sheff, A. Wierzbicki, J.H. Davis, R.D. Rogers, Chem. Commun. (2001) 135–136.
[31] J.H. Davis, Chem. Lett. 33 (2004) 1072–1077.
[32] Z. Wang, Q. Zhang, D. Kuehner, A. Ivaska, L. Niu, Green Chem. 10 (2008) 907–909.
[33] C. Chiappe, D. Pieraccini, D. Zhao, Z. Fei, P.J. Dyson, Adv. Synth. Catal. 348 (2006) 68–74.
[34] H. Itoh, K. Naka, Y. Chujo, J. Am. Chem. Soc. 126 (2004) 3026–3027.
[35] X.-D. Mu, J.-Q. Meng, Z.-C. Li, Y. Kou, J. Am. Chem. Soc. 127 (2005) 9694–9695.
[36] P. Dash, R.W.J. Scott, Chem. Commun. (2009) 812–814.
[37] V. Gallo, P. Mastrorilli, C.F. Nobile, G. Romanazzi, G.P. Suranna, J. Chem. Soc. Dalton Trans. (2002) 4339–4342.
[38] R. Narayanan, M.A. El-Sayed, J. Am. Chem. Soc. 125 (2003) 8340–8347.
[39] R. Narayanan, M.A. El-Sayed, J. Phys. Chem. B 109 (2005) 12663–12676.
[40] J. Durand, E. Teuma, F. Malbosc, Y. Kihn, M. Gomez, Catal. Commun. 9 (2008) 273–275.
[41] F. Fernandez, B. Cordero, J. Durand, G. Muller, F. Malbosc, Y. Kihn, E. Teuma, M. Gomez, Dalton Trans. (2007) 5572–5581.
[42] S. Jansat, J. Durand, I. Favier, F. Malbosc, C. Pradel, E. Teuma, M. Gomez, Chemcatchem 1 (2009) 244–246.
[43] L.S. Ott, R.G. Finke, Coord. Chem. Rev. 251 (2007) 1075–1100.
[44] S.-G. Lee, Chem. Commun. (2006) 1049–1063.
[45] H. Zhang, H. Cui, Langmuir 25 (2009) 2604–2612.
[46] J.R. Harjani, T. Friscic, L.R. MacGillivray, R.D. Singer, Inorg. Chem. 45 (2006) 10025–10027.
[47] M. Quinten, U. Kreibig, Surf. Sci. 172 (1986) 557–577.
[48] A. Stark, P. Behrend, O. Braun, A. Müller, J. Ranke, B. Ondruschka, B. Jastorff, Green Chem. 10 (2008) 1152–1161.
[49] L.C. Fidale, S. Köhler, M.G.H. Prechtl, T. Heinze, O.A. El Seoud, Cellulose 13 (2006) 581–592.
[50] J.P. Vivek, I.J. Burgess, J. Phys. Chem. C 112 (2008) 2872–2880.
[51] S.R. Isaacs, E.C. Cutler, J.-S. Park, T.R. Lee, Y.-S. Shon, Langmuir 21 (2005) 5689–5692.
[52] W. Cheng, S. Dong, E. Wang, Langmuir 19 (2003) 9434–9439.
[53] J.A. Creighton, D.G. Eadon, J. Chem. Soc. Faraday Trans. 87 (1991) 3881–3891.
[54] P. Dash, T. Bond, C. Fowler, W. Hou, N. Coombs, R.W.J. Scott, J. Phys. Chem. C 113 (2009) 12719–12730.
[55] J. Muzart, Tetrahedron 59 (2003) 5789–5816.
[56] S. Sato, R. Takahashi, T. Sodesawa, N. Yamamoto, Catal. Commun. 5 (2004) 397–400.